IDEALIZED SIMULATION OF AIRFLOW OVER A MOUNTAIN RIDGE USING A MESOSCALE ATMOSPHERIC MODEL

Assela PATHIRANA[1], Masafumi YAMAGUCHI[2], and Tadashi YAMADA[3]

[1]Member of JSCE, Ph.D.
[2]Student Member of JSCE, Graduate Student, Graduate School of Science and Engineering
[3]Member of JSCE, Ph.D., JSCE Corp.
Chuo University (1-13-27 Kasuga, Bunkyo-ku, Tokyo 112-8551, Japan)

In this paper the results of a number of idealized simulations of the airflow over a mountain ridge, using a fully compressible non-hydrostatic mesoscale atmospheric model is presented. First, the simulations were conducted with a steady background flow field as lateral boundary conditions. The results are interpreted with a special emphasis on formation and properties of lee waves and rotors. The effects of the changes in the atmosphere, topography and external wind field on lee wave and rotor properties are examined. It was found out that the flow fields generated by the present model are significantly different and much more complicated than those predicted by the linear theories. Most of the conditions produced single or multiple rotors that caused boundary layer separation on the lee side. Secondly, the effect of unsteadiness of the background flow on the lee wave dynamics was examined. It was found out that a gradual drop of wind speed could cause the lee wave train to move upstream and to cause a considerable rotor-like motion over the mountain ridge. An attempt is made to link this behavior of the model under the unsteady wind with the observed abundance of thunderstorm activities over mountain ridges compared with surrounding lowlands.

Keywords: *mesoscale atmospheric model, lee waves, rotor, thunderstorm*

1. Introduction

Dynamics of wind fields moving over orthogonal mountain ridges have been studied for a long time using increasingly sophisticated techniques. Most of the early theoretical studies used linear theories to explain the behavior of trapped lee waves that occur as a result of these flows. However, the amplitudes of observed lee waves are usually sufficiently large, so that non-linear effects dominate (Pilke 2002)[1)]. Recent years have seen a number of studies of lee wave behavior using non-linear dynamics of the atmospheric motion.

Yamada et al (1994)[2)] used linear theory (frequency domain analysis) to study the flow above a ridge. They investigated the range of internal Froude number that generates trapped lee waves. They also reported that the flows with small internal Froude numbers that are not strong enough to flow above the ridge top, generates stagnation points on the lee-side.

In this paper, we present a modeling study of mountain induced lee waves using the Pennsylvania State University's MM5[3)] modeling system. The original model was modified to make it possible to run the system with idealized boundary and initial conditions. A number of simulations with varying parameters were performed. The sensitivity of the lee wave structure to the topography, atmospheric condition and flow velocity was investigated. A preliminary explanation for the large concentrations of lightning activities over the mountain ranges surrounding Kanto-plains is attempted using the insights from the analysis of lee wave behavior under unsteady external wind fields.

2. Selection of the Modeling System

MM5 is a 3-dimensional mesoscale model with fully compressible non-hydrostatic dynamics, which is widely used to perform limited area atmospheric simulations for operational use and research. The model requires the specification of the initial conditions all over the modeling domain and the lateral boundary conditions during the whole time period of simulation. Boundaries need to have specified horizontal winds, temperature, pressure and moisture conditions and optionally microphysical fields. In an operational scenario, the lateral boundary data are usually obtained from a global scale model results or analyses at some intermediate spatial scale, which ultimately depend on a global model. In historical studies lateral boundary conditions can be enhanced using observational data. Performing idealized simulations is not a standard usage of the model and therefore a number of additional modifications are needed before the model can be used for the purpose similar to the one of the present research. However,

there are a number of distinct advantages in using MM5 as the basis for an idealized study. The modeling system is used for operational modeling at a number of organizations in the world, resulting in a well-tested numerical system. The model source is freely available for use. Further, due to the model's ability to perform simulations based on real observational data and large-scale model outputs with relative ease, it is feasible to extend the ideal simulations to those using real data in future research, without switching to a different mesoscale model.

2.1. Governing equations

The vertical scale of the MM5 model is defined by the dimensionless coordinate σ.

$$\sigma = (p - p_t)/(p_s - p_t) \qquad (1)$$

Where *p* is the pressure, subscripts *t, and b* indicate model top and ground surface, respectively. Atmospheric data is typically input in pressure surfaces and are internally interpolated in to σ coordinates.

Basic equations in terms of terrain following coordinates (*x*, *y*, σ) used in the model are shown bellow.

$$\frac{\partial p'}{\partial t} - \rho_0 g w + \gamma p \nabla \cdot \mathrm{V} = -\mathrm{V} \cdot \nabla p' + \frac{\gamma p}{T}\left(\frac{\dot{Q}}{c_p} + \frac{T_0}{\theta_0} D_\theta\right)$$

(Non-hydrostatic pressure) (2)

ρ is density of atmosphere, *g* is gravitational acceleration, c_p is the specific heat at constant pressure, $\gamma = c_p / c_v$ where c_v is the specific heat at constant volume, T absolute temperature, Q heat, and θ potential temperature. The pressure P is broken-down to $P = P_o + P'$ where $P_o \approx \rho_o g z$ is the hydrostatic pressure and P' perturbation of the actual (non-hydrostatic) pressure from that.

$$\frac{\partial u}{\partial t} + \frac{m}{\rho}\left(\frac{\partial p'}{\partial x} - \frac{\sigma}{p^*}\frac{\partial p^*}{\partial x}\frac{\partial p'}{\partial \sigma}\right) = -V \cdot \nabla u$$

$$+ v\left(f + u\frac{\partial m}{\partial y} - v\frac{\partial m}{\partial x}\right) - ew\cos\alpha - \frac{uw}{r_{earth}} + D_u \qquad (3)$$

$$\frac{\partial v}{\partial t} + \frac{m}{\rho}\left(\frac{\partial p'}{\partial y} - \frac{\sigma}{p^*}\frac{\partial p^*}{\partial y}\frac{\partial p'}{\partial \sigma}\right) = -V \cdot \nabla v$$

$$+ u\left(f + u\frac{\partial m}{\partial y} - v\frac{\partial m}{\partial x}\right) - ew\sin\alpha - \frac{vw}{r_{earth}} + D_v \qquad (4)$$

$$\frac{\partial w}{\partial t} + \frac{\rho_o}{\rho}\frac{g}{p^*}\frac{\partial p'}{\partial \sigma} + \frac{g}{\gamma}\frac{p'}{p} = -V \cdot \nabla w + g\frac{p_o}{p}\frac{T'}{T_o} - \frac{gR_d}{c_p}\frac{p'}{p}$$

$$- e(u\cos\alpha - v\sin\alpha) + \frac{u^2 + v^2}{r_{earth}} + D_w \qquad (5)$$

where m is a scale-factor, $p^* = p_s - p_t$, f is a dimensionless quantity representing friction, r_{earth} is radius of the earth. Equation (3)-(5) represent the three spatial components of momentum. Third term on the right represents Coriolis force, where $e = 2\Omega\cos\lambda$, $\alpha = \phi - \phi_c$, λ is altitude, ϕ is longitude.

$$\frac{\partial T}{\partial t} = -V \cdot \nabla T + \frac{1}{\rho c_p}\left(\frac{\partial p'}{\partial t} + V \cdot \nabla p' - \rho_0 g w\right)$$

$$+ \frac{\dot{Q}}{c_p} + \frac{T_0}{\theta_0} D_\theta \quad \text{(Thermodynamics)} \qquad (6)$$

Microphysics was neglected in the present study.

2.2. Modifying MM5 for ideal simulations

In order to perform idealized simulations the first step is to device a means of specifying idealized initial and boundary conditions. Leutbecher (1996)[4] has written two preprocessing modules named TERRAINI and DATAGRIDI to support ideal simulations with MM5 on Cray super computer systems. In the present research the ideal simulations were based on these modules, modified to run on a personal computer running Linux operating system.

The original DATAGRIDI program was written to generate wind fields with velocities constant in time. The code was modified to make it possible to specify variable wind fields. Such modification was needed to run the model with a wind field starting at zero velocity, gradually increasing to the prescribed velocity with time (within an hour) and then remains constant for a reasonable duration. Such gradual start is needed to avoid spurious gravity waves that occur due to a sudden start of the wind. Doyle and Durran (2001)[5] suggest a similar gradual increase in gravitational acceleration also, but in the present study such a modification was not done.

A flowchart of the model components used is shown in Fig. 1.

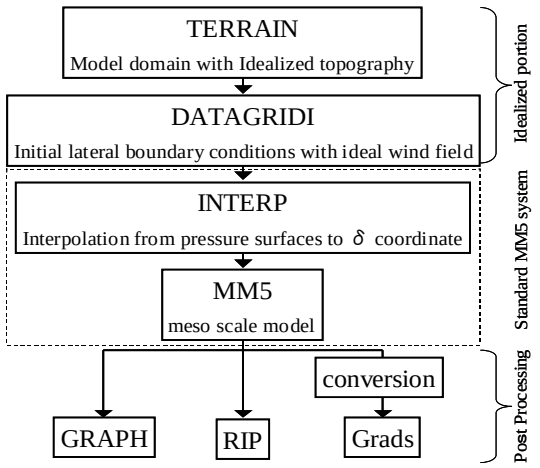

Fig. 1 A flow chart of MM5 model setup for idealized simulations

3. Lee waves

Lee waves occur under certain conditions when wind blows in a stably stratified atmosphere (potential temperature increasing with height) over a mountain ridge. The linear theory states that well-developed lee waves occur when the Scorer parameter (S_0), defined below, decreases with altitude.

$$S_0 = \frac{N^2}{U^2}$$

Where $N = \sqrt{g\partial \ln(\theta)/\partial z}$ is the Brunt-väisälä frequency, U is the velocity of the flow field, θ is potential temperature, g is gravitational acceleration and z is the altitude. Therefore, there are two situations where lee waves can occur, namely 1) when the stability decreases with the height, 2) when the flow velocity increases with height. In the present paper the former condition, namely, decreasing stability-stability and constant velocity with elevation, is examined. Another important quantity that can characterize fluid flow over a ridge in the Froude Number defined by $F_r=V_g/(z_{Gmax}N)$ where V_g is the large-scale velocity over the ridge and z_{Gmax} is the maximum height of the ridge (Pilke 2002).[1)]

Reported observational studies on lee waves using various means like weather radar and aircraft measurements include Holmboe and Klieforth (1957)[6)], Colson and Lindsay (1959)[7)], Lindsay (1962)[8)], Brown (1983)[9)] and Ralph et al (1997)[10)].

Doyle and Durran (2001)[5)] used the two-dimensional version of the Coupled Ocean-Atmospheric Mesoscale Prediction System (COAMPS) developed by U.S. military to investigate the dynamics of rotors associated with the lee waves. They observed that there is a threshold value of ridge height, only above which the flow separation due to rotors will occur. Nance and Durran (1997,1998)[11)12)] investigated the effects of unsteady background flow on lee wave behavior using a fully compressible model developed by Durran and Klemp (1983)[13)].

4. Numerical experiment

A particularly simple atmosphere with two layers (with interface at a 3km height from the base) was used for the experiments reported in this paper. The single mountain ridge included was a one with a Gaussian profile of a uniform height h and width parameter of 8km (Fig. 2).

For economy in computing a nested grid system (Fig. 3) was used to represent the horizontal domain. Vertical grid spacing was minimum near the surface and was increased with height. Due to the incorporation of sound waves in the MM5 model, the finite difference scheme had to be solved at rather a small time step of 6s (for outer domain. Inner domain was solved at $\Delta t = 2$ s). The MRF-PBL scheme with roughness of 0.1m was used to represent the planetary boundary layer.

The above model configuration was run in a personal computer with Intel Pentium IV processor of 1.7GHz, running RedHat Linux operating system version 7.3. Compiled with Portland Groups compilers, simulation of 8h took about 6h of computing time.

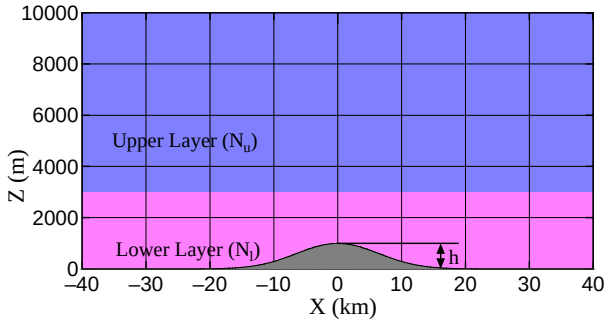

Fig. 2 Model setup. N_u and N_l indicate the Brunt-väisälä frequency of the upper and lower layers. Mountain profile is defined by $z = h\exp(-x^2/b^2)$, where h is the maximum height.

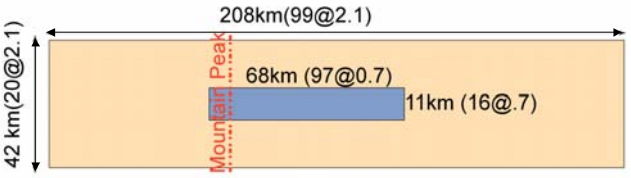

Fig. 3 Numerical setup. A high-resolution (0.7km) grid of 97x16 was nested inside the coarser (2.1km) grid of 99x20. Vertical space was divided in to 50 grids with unequal spacing.

5. Simulations

Each simulation was started with almost zero wind and then the wind velocity was gradually increased to reach the prescribed velocity in an hour. Then the simulation was continued until steady conditions are achieved. Usually the model dynamics becomes steady after about 5-6h. The results reported here were obtained at t=8h.

5.1. Simulation 1

A highly stable atmosphere (with a temperature inversion at the bottom layer) with N_u=.01 and N_l=.025 was used for the first set of simulations. Keeping the mountain height at 1000m, the wind speed was varied from 10m/s to 50m/s in steps of 5m/s. For this atmospheric configuration the velocities below 20m/s did not produce trapped lee waves. Instead the waves propagated vertically or slanted (e.g. see Fig. 4). Formation of lee-side rotors were observed for all velocities except 25m/s. Velocities 35, 40, 45m/s produced multiple rotors (Fig. 5). Up to 45m/s there was a distinct difference of the wavelengths of the waves in upper and lower layers. For velocities above that, the atmosphere seems to behave like that of a single layer

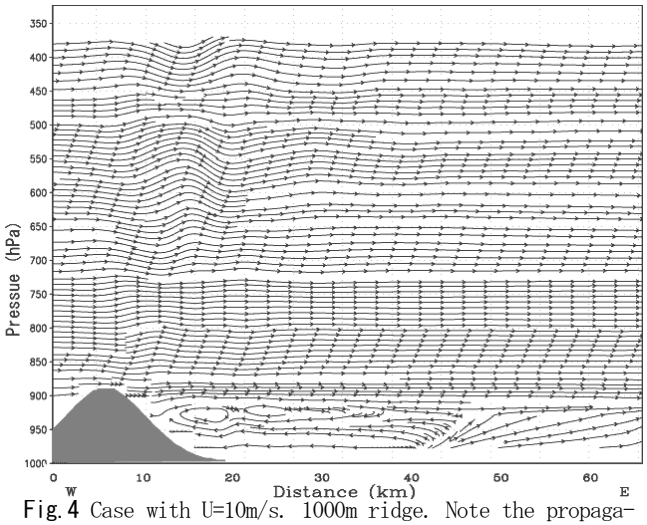

Fig.4 Case with U=10m/s. 1000m ridge. Note the propagation of lee waves almost vertically upwards. In this case the waves are not trapped. F_{ru}=1, F_{rl}=0.4

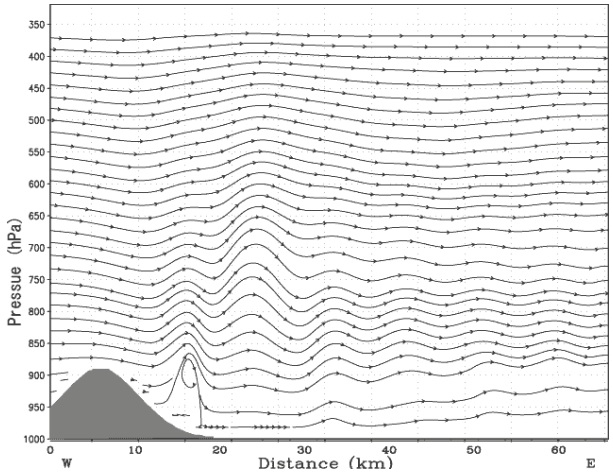

Fig.5 Lee wave train generated for 35m/s case with 1000m ridge(Streamlines). F_{ru}=3.5, F_{rl}=1.2.

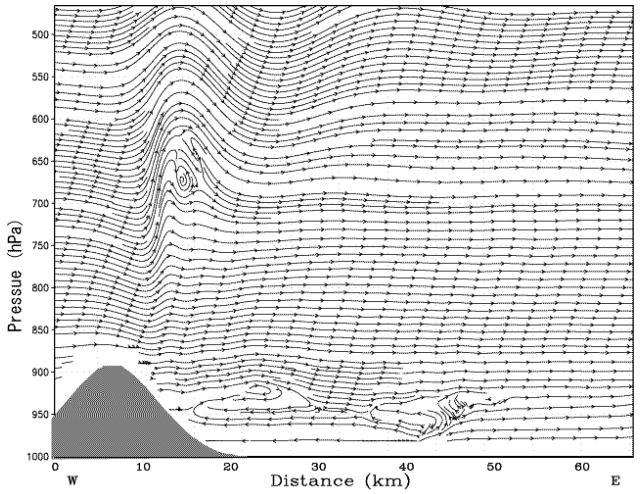

Fig.6 Streamlines for the 25m/s, 1200m ridge height case. In addition to the rotor beyond the lee slope, there is a vortex above the lee-side slope also. F_{ru}=2.1, F_{rl}=0.8

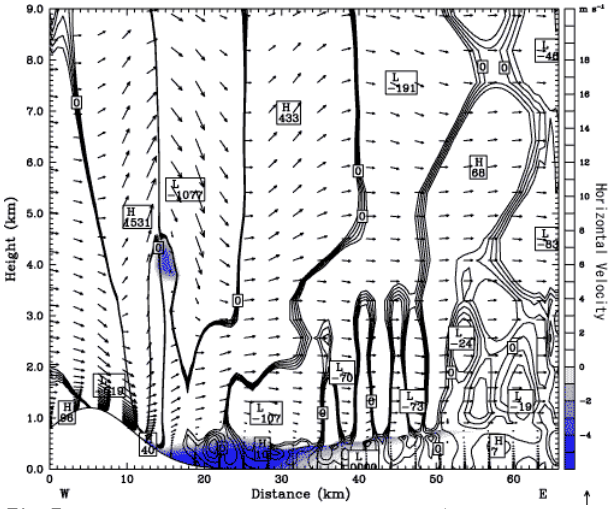

Fig.7 Velocity vectors for 1200m 25m/s case. Contours: vertical velocity (cm/s). Shading: horizontal velocity (only negative values are emphasized).

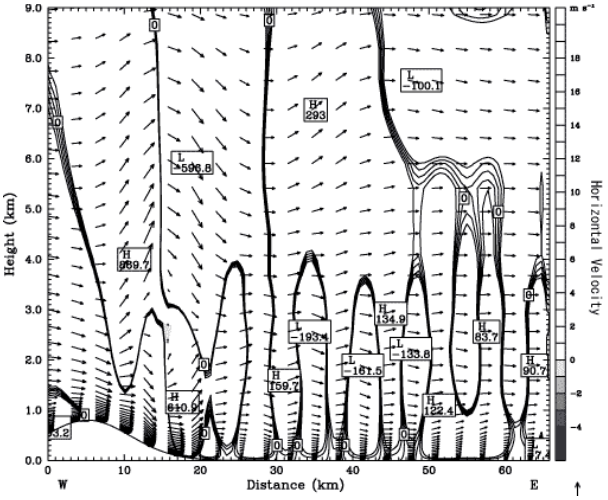

Fig.8 Velocity vectors for 800m 25m/s case. Contours: vertical velocity (cm/s). Shading: horizontal velocity (only negative values are emphasized).

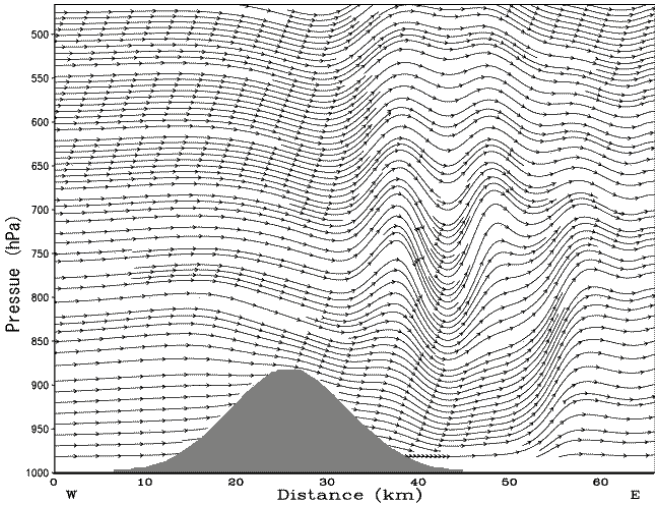

Fig.9 Streamlines for the case with 10m/s, just before start of the decreasing the wind to 5m/s. F_{ru}=2.1, F_{rl}=1.3.

producing a single wavelength in both layers. The results are summarized in Table. 1.

Another series of experiments were conducted by keeping background flow constant at 25m/s and varying the height of the mountain from 200m to 2000m. Mountains higher than 1000m did not produce strong lee waves (Fig. 6). However, by examining the vertical velocity contours it was possible to identify a lee wave like behavior further downstream (Fig. 7). There were large stagnation areas on the lee side plain. The 800m (Fig. 8) and 1000m mountains produced strong lee wave patterns. The 200m and 400m topographies were not adequate to generate strong lee waves.

Table 1: Summery of simulations with different background flows (h=1000m)

Velocity m/s	10*	15**	20	25	30	35	40	45	50
Froude Number (Upper)	1	1.5	2	2.5	3	3.5	4	4.5	5
Wave Length (Upper) km	x	13	20	30	30	37	38	15	18
W.L from Classical theory km	6	9	13	16	19	22	25	28	31
Froude Number (Lower)	0.4	0.6	0.8	1.0	1.2	1.4	1.6	1.8	2.0
Wave Length (Lower) km	x	x	x	6	7	7	11	15	18
W.L from Classical theory km	3	4	5	6	8	9	10	11	13
Rotor Formation	●	●	●	x	●	●	●	●	●
Multiple Rotors	x	x	x	x	x	●	●	●	x
* wave propergates vertically	**	Wave propergates slanted					x	No lee waves	

Table2: Simulation with variable mountain height (U=25m/s)

Mountain Height (100m)	2	4	8	10	12	16	20
Froude Number (Upper)	12.5	6.3	3.1	2.5	2.1	1.6	1.3
Wave Length (Upper) km	30	30	30	30	25	15	15
Froude Number (Lower)	5.0	2.5	1.3	1.0	0.8	0.6	0.5
Wave Length (Lower) km	8	10	7	6	7	5	4
Rotor at lee-side Mountain Foot	x	x	x	x	●	●	●
Rotor above lee-slope	x	x	●	●	●	●	●
* wave propergates vertically	**	Wave propergates slanted					

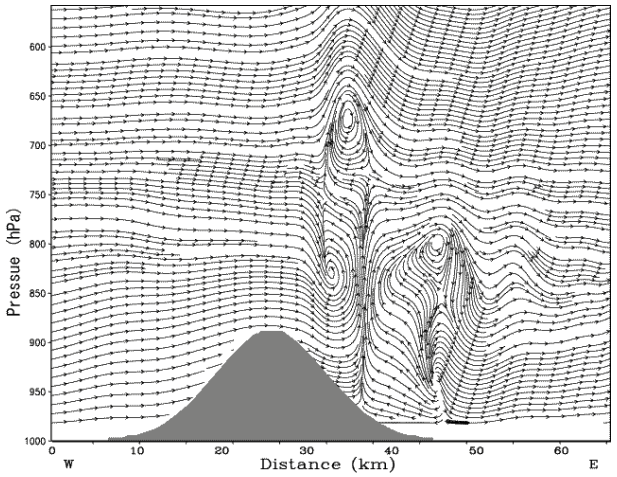

Fig. 10 Streamlines at 1h after transition of background flow from 10m/s to 5m/s. F_{ru}=1.3, F_{rl}=0.6

5.2. Simulation 2

Background flows in many actual atmospheric situations where lee waves occur, can hardly be explained as steady (Vergeiner and Lilly (1970) [14], Mitchell et al. (1990) [15]). Transitional nature of background flow may have a considerable effect on the formation and nature of lee waves. In order to examine this situation a series of simulations with the following conditions were performed. Once the dynamics are stabilized under a constant background flow as in the previous experiment, the velocity of wind is changed to a different value within a specified time interval. Only a single case of particular interest will be presented here. In this case N_u=.00387 and N_l= .00775 was selected following the (linear) theoretical studies by Scorer (1949) [16]. After the system was stabilized under a wind speed of 10m/s (Fig. 9), the background flow was reduced to 5m/s within a period of 1h. Then the system was run further with the new wind speed.

The most interesting result of this simulation is the finding that the lee wave starts to move upwind while and after the velocity is being reduced. The lee wave train does not proceed beyond the peak of the mountain but instead forms large turbulence above the peak of the mountain (Fig. 10).

6. Discussion:

The numerical experiments show a number of interesting features of the atmospheric flow over a mountain ridge. Results of non-linear simulations are significantly different from those obtained from classical (linear) theory. Characteristics of the lee waves formed seem to be governed by many factors like the wind speed, size of the mountain ridge and atmospheric properties. Boundary layer separation caused by rotor formation on the lee-side was observed in almost all cases. When the mountain height is increased beyond about 1000m, the strength of lee waves diminished greatly and stagnation areas of increasingly larger extent were formed on the lee side.

The rotor formed over the mountain ridge approximately at 600-700hPa levels in simulations with mountain height above 800m (see Table. 2, Fig. 6 and Fig. 7) was a feature that was not reported by previous modeling studies. However, at this stage it is not definite whether this is a real phenomenon or an artifact of the two-layer atmosphere model used in the simulation. In real atmospheric situations, the static stability does not drop abruptly at a particular level, so that it may be possible that this type of rotors does not occur in the real atmosphere. The classical theory relates only the width of the topography to the conditions needed for formation of trapped lee waves. However, the present simulations show that the lee waves do not occur above and below the 800m – 1000m range, for the atmospheric conditions specified. Further, for the same conditions, rotor formation occur only with mountains higher than 1000m. This observation is qualitatively in agreement with the results of Doyle and Durran (2001) [5], though the threshold reported there was much smaller (400m).

Decreasing of the background flow caused the lee wave train to move upstream. A number of observers have noted the presence of waves in the wind side of a mountain ridge (Clark

et al, 1982[17]). However, in the present study the lee waves did not move beyond the peak of the mountain. Instead they formed strongly-disturbed region above the ridge peak. We propose that these disturbances might be one of the possible explanations for the increased thunderstorm activities over mountain ranges compared with the surrounding plains. One such example is the marked increase of lightning over the North Western mountain ridges of the Kanto Plain. Fig. 11 shows the locations of generation points of thunderstorms in Kanto Plains and the nearby mountains. These locations were derived from the radar observations made by the Dopplar radar of the Chuo University (whose location is shown by a cross). The instantaneous rainfall intensity over 32mm/hr was defined as thunderstorms. The Ashio and Chichibu mountain ranges show a significantly larger density of generation points than the plain areas. It is intended to extend the present study in this direction to examine whether there is a definite relationship between unsteady lee wave generated turbulence and the increase of lightning activities.

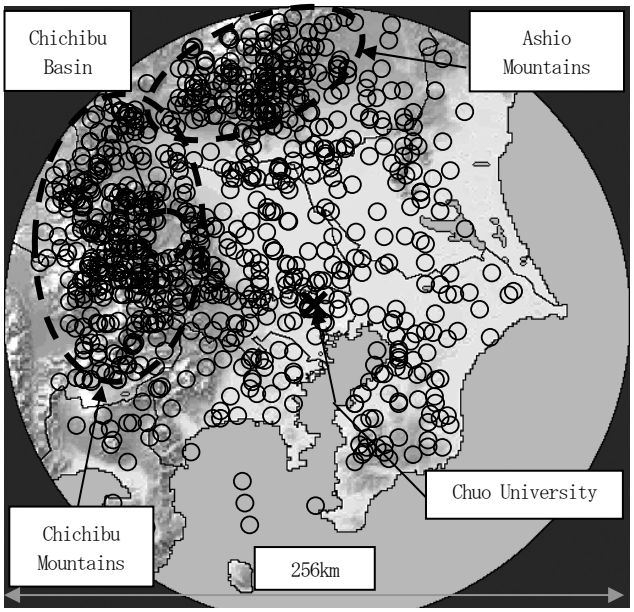

Fig. 11 Generation points of thunderstorms in the Kanto Plain.

Reference:

1) Pilke R, Mesoscale Meteorological Modeling, 2nd ed., Academic Press, 2002.
2) Yamada, T., Hibino, T., Fukawa, G., and Nakatugawa, M.: Analysis of wind field considering the effect of stratified atmospheric in mountain area, Ann. J. Hydr. Engrg, JSCE, vol. 38, pp. 13-18, 1994. (in Japanese with abstract in English)
3) PSU/NCAR Mesoscale modeling system tutorial class notes and user's guide: MM5 modeling system version 3, Mesoscale and Microscale Meteorology Division, National Center for Atmospheric Research (NCAR), 2002.
4) Leutbecher, M.:, Terraini and Datagridi, ftp://ftp.ucar.edu/mesouser/user-contrib/ideal.tar.gz, 1996.
5) Doyle J. D., and Durran. D. R.: The dynamics of Mountain-wave-induced rotors, *J. Atmos. Sci.*, 59, 186-201, 2001.
6) Holmboe, J., and H. Klieforth: Investigation of mountain lee waves and airflow over the Sierra Nevada., Final Rep. Contract AF19(604)-728, University of California ADNo. 133606, Department of Meteorology, University of California, Los Angels, 290 pp., 1957.
7) Colson, D., and C. V. Lindsay: Unusual wave cloud over Washington DC, *Mon. Wea. Rev.*, 87, 451-452, 1959.
8) Lindsay, C. V.: Mountain waves in the Appalachians, *Mon.Wea. Rev.*, 111, 430-444, 1962.
9) Brown, P. R. A.: Aircraft measurement of mountain waves and their associated momentum flux over British Isles, *Quart. J. Roy. Meteor. Soc.*, 109, 849-865, 1983.
10) Ralph, F. M., J. Neiman, T. L. Keller, D. Levinson, and L. Fedor: Observations, simulations and analysis of nonstationary trapped lee waves, *J. Atmos. Sci.*, 54, 1308-1333, 1997.
11) Nance, L.B., and D.R. Durran. : A modeling study of nonstationary trapped mountain lee waves, Part I: Mean flow variability. *J. Atmos. Sci.*, 54, 2275-2291, 1997.
12) Nance, L.B., and D.R. Durran: A modeling study of nonstationary trapped mountain lee waves, Part II: Nonlinearity. *J. Atmos. Sci.*, 55, 1429-1445, 1998.
13) Durran, D.R., and J.B. Klemp: A compressible model for the simulation of moist mountain waves, *Mon. Wea. Rev.*, 111, 2341-2361, 1983.
14) Vergeiner, I., and D. K. Lilly: The dynamic structure of lee wave flow as obtained from balloon and airplane observations, *Mon. Wea. Rev.*, 1970, 220-232
15) Mitchell, R. M., R. P. Cechet, P. J. Turner, and C. C. Elsum: Observation and interpretation of wave cloud over Macquarie Island, *Quart. J. Roy. Meteor. Soc.*, 116, 741-752. 1990.
16) Scorer, R.S.: Theory of waves in the lee of mountains, *Quarterly Journal of the Met Society*, Vol 75, 41-56. , 1949.
17) Clark, T. L., and R. Gall. : Three-dimensional numerical model simulations of airflow over mountainous terrain: A comparison with observations, *Mon. Wea. Rev.*, 110, 766-791, 1982.

(Received October 30, 2002)